Chemosphere 240 (2020) 124961

Contents lists available at ScienceDirect

Chemosphere

journal homepage: www.elsevier.com/locate/chemosphere

# Metabolic response of vetiver grass (*Chrysopogon zizanioides*) to acid mine drainage

Jeffrey D. Kiiskila [a], Kefeng Li [b], Dibyendu Sarkar [c], Rupali Datta [a, *]

[a] Department of Biological Sciences, Michigan Technological University, Houghton, MI, USA
[b] School of Medicine, University of California, San Diego, CA, USA
[c] Department of Civil, Environmental and Ocean Engineering, Stevens Institute of Technology, Hoboken, NJ, USA

## HIGHLIGHTS

- Exposure to AMD lead to differential metabolic shift in vetiver root and shoot.
- Combined abiotic stress from AMD lead to nutrient derivation and oxidative stress.
- Shoot displayed increased amino acid, glutathione, TCA and urea cycle metabolism.
- Root showed downregulation of amino acid, nucleic acid and glyoxylate metabolism.
- Downregulation of phosphorylated metabolites was observed in both root and shoot.

## GRAPHICAL ABSTRACT

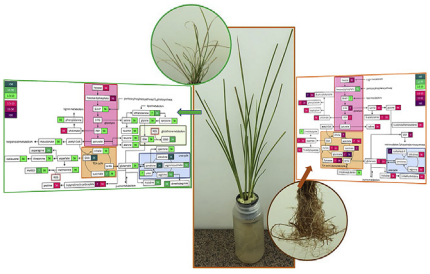

## ARTICLE INFO

*Article history:*
Received 16 May 2019
Received in revised form
9 September 2019
Accepted 23 September 2019
Available online 24 September 2019

Handling Editor: T Cutright

*Keywords:*
Acid mine drainage
Heavy metals
Phytoremediation
Vetiver grass
Combined abiotic stress
Metabolomics

## ABSTRACT

Acid mine drainage (AMD) is a sulfuric discharge containing metals and particulates that can spread to nearby water sources, imposing toxicity and physical stress to living things. We have shown that vetiver grass (*Chrysopogon zizanioides*) is capable of tolerating and treating AMD-impacted water from the abandoned Tab-Simco mining site from southern Illinois, though little is known about its tolerance mechanisms. We conducted metabolomic analyses of vetiver shoots and roots after relatively short- and long-term periods of exposure to Tab-Simco AMD. The metabolic shift of vetiver shoots was dramatic with longer-term AMD exposure, including upregulation of amino acid and glutathione metabolism, cellular respiration and photosynthesis pathways, with downregulation of phosphorylated metabolites. Meanwhile, the roots demonstrated drastic downregulation of phospholipids and phosphorylated metabolites, cellular respiration, glyoxylate metabolism, and amino acid metabolism. Vetiver accumulated ornithine and oxaloacetate in the shoots, which could function for nitrogen storage and various intracellular functions, respectively. Organic acids and glutathione were secreted from the roots for rhizospheric metal-chelation, whereas phosphorylated metabolites were recycled for phosphorus. These findings reveal AMD-induced metabolic shifts in vetiver grass, which are seemingly unique in comparison to independent abiotic stresses reported previously.



* Corresponding author.
*E-mail address:* rupdatta@mtu.edu (R. Datta).

https://doi.org/10.1016/j.chemosphere.2019.124961
0045-6535/

## 1. Introduction

Acid mine drainage (AMD) is formed due to the oxidation of iron pyrite and other sulfidic minerals exposed to water and oxygen due to mining operations. Under these conditions, the minerals release Fe, $SO_4^{2-}$ and $H^+$ (RoyChowdhury et al., 2015). AMD is highly acidic and contains high concentrations of metals, although its chemical characteristics are variable and a function of the local mineralogy (Hogsden and Harding, 2012). AMD poses major health and environmental concerns by contaminating water sources, which results in reduced biodiversity and biomagnification (RoyChowdhury et al., 2015). Metal hydroxides in AMD accumulate as orange-yellow precipitates (RoyChowdhury et al., 2015; Hogsden and Harding, 2012), which can also harm living organisms through physical stress (Hogsden and Harding, 2012).

Several plants have been screened for AMD tolerance, e.g., *Typha latifolia*, *Scirpus validus*, etc. (Karathanasis and Johnson, 2003; Ma et al., 2015). Plants remove metals through root uptake and/or precipitation (Pardo et al., 2016), which may accumulate as root plaques composed of metal hydroxides (Li et al., 2017b). Vetiver grass, *Chrysopogon zizanioides*, is a noninvasive and fast-growing perennial grass that tolerates and accumulates metals (Andra et al., 2009; Pidatala et al., 2018; Kiiskila et al., 2019). Vetiver can grow sustainably in hydroponics (Andra et al., 2009; Pidatala et al., 2018; Kiiskila et al., 2019), including acidic waters like AMD (RoyChowdhury et al., 2015; Kiiskila et al., 2019). Moreover, vetiver has massive, self-regenerating roots that can form plaques and sequester metals (Kiiskila et al., 2019).

Our ultimate goal is to develop a floating treatment wetland using vetiver for the remediation of AMD. A shorter-term, bench-scale experiment using AMD from the Tab-Simco coal mining site near Carbondale, Illinois demonstrated that vetiver can effectively increase pH in AMD while reducing $SO_4^{2-}$ and metals within 30 days (Kiiskila et al., 2017). A longer-term, follow-up study demonstrated more significant changes in pH ($\geq$3.4), $SO_4^{2-}$, and decline in metals at both mesocosm and microcosm levels (Kiiskila et al., 2019). Vetiver has been well characterized for its response to AMD; however, little is known about its biochemical tolerance mechanisms to this complex medium. Metabolomics is invaluable for understanding plant stress as it provides large datasets that are not dependent on genetic information (Pidatala et al., 2016).

Single factors such as individual metals have been the focus of abiotic stress research; however, plants experience multiple stresses in the environment (Mittler, 2006; Sun et al., 2015; Li et al., 2017a; Martinez et al., 2018). Previously, we evaluated vetiver and maize for their metabolomic responses to individual metals, particularly Pb and Cu (Li et al., 2014; Pidatala et al., 2016, 2018). To the best of our knowledge, systems-based approaches like metabolomics or proteomics have not been applied to evaluate plant responses to the combined stresses of AMD. Combined stresses have come under recent investigation for agricultural purposes, often revealing that they have more severe impacts than individual stresses (Li et al., 2017a). Furthermore, plants have demonstrated unique metabolic shifts and expression patterns that are incomparable to individual stresses (Mittler, 2006; Sun et al., 2015; Li et al., 2017a; Martinez et al., 2018), which could provide critical insights for biotechnological advancements (Martinez et al., 2018).

In this paper, we report a metabolic profiling study of vetiver grass exposed to Tab-Simco AMD over shorter- and longer-term periods to understand their tolerance mechanisms. Vetiver was simultaneously evaluated for physiological responses such as effect on growth, metal uptake and accumulation.

## 2. Materials and methods

### 2.1. Hydroponic experiments and sample acquisition

AMD was collected from the Tab-Simco site for remediation experiments (Kiiskila et al., 2019). Vetiver (Sunshine variety) was acclimated in media (0.5X Hoagland's solution) for two months, and transferred into light-shielded LDPE bottles containing 450 mL of AMD for treatment or fresh media for comparison (Kiiskila et al., 2017). Plants were grown for 7 and 56 days (n = 6 plants) to compare vetiver response to shorter and longer-term exposure to AMD. Bottles of AMD without plants were used as control. Deionized water was used to replenish water loss from transpiration and evaporation; pH was not adjusted. Plants were measured for fresh biomass before and after the experiments. Samples for metabolomics were flash frozen using liquid nitrogen (n = 3 plants) and stored at −80 °C. Dissolved oxygen was measured as described in Kiiskila et al. (2019). For analysis of exuded metabolites, light-shielded 250 mL beakers containing 100 mL of AMD were used to grow vetiver for 7 days in replicates of n = 3, along with plant-free beakers for control. Water was flash frozen and stored at −80 °C for metabolite analysis.

### 2.2. Water characterization and plant measurements

Water was screened for pH, soluble ions ($SO_4^{2-}$, $NO_3^-$) and metals as described in Kiiskila et al. (2019). Total chlorophyll was analyzed following Arnon (1949) using the following equation: $Total\ Chlorophyll = (20.2\ x\ A_{645} + 8.02\ x\ A_{663})\ x\ dilution\ factor$. Tissues were digested and evaluated for metals as described in Kiiskila et al. (2019).

### 2.3. Metabolite extractions and LC-MS/MS

Plants were divided into roots and shoots, and homogenized into fine powder using liquid nitrogen. Metabolite extractions followed De Vos et al. (2007) with slight modifications (Pidatala et al., 2018). AMD was thawed to 4 °C and syringe filtered (0.22 μm). 100 μL subsamples of AMD were treated with 400 μL of methanol:acetonitrile (1:1) for 10 min at 4 °C, centrifuged (16,000 rcf) for 10 min, and the supernatant was dried for metabolite analysis. Metabolites were analyzed by LC-MS/MS as described in Pidatala et al. (2016) with a Shimadzu UFLC XR HPLC System (LC-20AD Model) and a SCIEX 5500 QTRAP MS with Turbo V Electrospray Ionization (ESI) Source. 248 metabolites were targeted covering primary metabolic pathways. Chromatographic peaks were manually inspected and integrated using MultiQuant 3.0 software (SCIEX, USA). Peak areas were exported to excel and max/min analysis was performed to ensure data quality.

### 2.4. Data processing and statistical analysis

Changes in water and plant measurements were compared using two-sample t-tests with JMP® Pro 13 software ($p < 0.05$). Metabolites were processed using MetaboAnalyst 3.0 (www.metaboanalyst.ca), replacing missing values by the k-NN method and normalizing data through log2 transformation with autoscaling. Metabolites were compared by fold change ($\geq$1.5 threshold) with FDR adjusted t-testing ($p < 0.05$).

## 3. Results and discussion

### 3.1. Evaluation of vetiver in response to AMD

Tab-Simco AMD contained high concentrations of five soluble metals (Fe, Al, Mn, Zn and Ni) and one insoluble metal (Cr) (Table 1A). On treatment with vetiver, AMD showed a slight increase in pH at 7 days along with decreases in dissolved oxygen and $SO_4^{2-}$ (Table 1A). Greater changes were observed at 56 days, including an increase in pH from 2.43 to 3.23 ($p = 0.010$). Additionally, $SO_4^{2-}$ decreased at 56 days from 400 mg $L^{-1}$ to 166 mg $SO_4^{2-}$ $L^{-1}$ ($p < 0.001$), and Fe decreased from 64,500 μg $L^{-1}$ to 6550 μg $L^{-1}$ ($p = 0.002$). Excluding Cr, all metals decreased at 56 days in plant treated AMD ($p \leq 0.006$) but not as significantly as Fe. The change in the media was less significant, though dissolved oxygen, $SO_4^{2-}$, and $NO_3^-$ decreased (Table 1A).

AMD impacted vetiver growth, with plants showing decreased biomass by 27.3% compared to the initial biomass, while the biomass of media-grown vetiver decreased by 2.92% at 7 days ($p = 0.001$, Table 1B). AMD-grown shoots demonstrated some drying, browning, and curling at the blade tips (Fig. 1). Chlorophyll content was lower in AMD-grown shoots (1.28 mg $g^{-1}$) compared to that of media-grown shoots (2.62 mg $g^{-1}$) ($p = 0.007$). Furthermore, R:S ratios increased from 0.30 in media-grown vetiver to 0.47 in AMD-grown vetiver ($p = 0.040$) where brown-orange plaques accumulated along the root surfaces (Fig. 1).

AMD-grown biomass decreased 30.2% at 56 days, but increased 31.7% in media ($p < 0.001$) (Table 1B). Despite drying of the shoots, fresh growth with comparable chlorophyll to media-grown plants was observed. Moreover, flakey white solids accumulated around the base of the shoots. Plaque development started at the root-shoot transition and gradually extended to the tips while fresh growth emanated from the transition with no significant difference in R:S ratios. AMD-grown vetiver accumulated > 2-fold metals at 7 days and > 3-fold at 56 days with variable translocation (Table 1C). Fe and Cr were held in the roots while Mn and Ni were translocated.

Heavy metals are known to displace essential metals in biological systems and cause macromolecular interference (Hossain et al., 2012; Das and Roychoudhury, 2014; Liang et al., 2016). Redox active metals such as Fe, Mn and Cr produce reactive oxygen species or ROS (Hossain et al., 2012), which results in inhibited growth (Hossain et al., 2012; Xie et al., 2014; Liang et al., 2016), decreased photosynthesis, chlorosis, and turgor loss in vetiver (Hossain et al., 2012; Xie et al., 2014).

At low pH, protons generate oxidative stress, which likely damaged the outer layers of vetiver roots, depolarizing membranes, and interfering with growth and root elongation (Koyama et al., 2001; Lager et al., 2010; Shavrukov and Hirai, 2016). Koyama et al. (2001) reported irreversible damage in actively growing roots of *Arabidopsis thaliana* at low pH, but no such damage was

**Table 1**
(A) Characteristics of Tab-Simco AMD and media at 7 and 56 days, including untreated AMD (UA), treated AMD (TA), untreated media (UM), and treated media (TM). **(B)** Characteristics of vetiver grass after 7 and 56 days in AMD (or media), including root-to-shoot (R:S) ratios (**C**) metal contents of vetiver shoots (S) and roots (R) per dry plant mass. Represented are mean ± standard deviation for n = 3 replicates.

A) Characteristics of Tab-Simco AMD and media

| Treatment | Time (days) | pH | Ions (mg $L^{-1}$) | | Metals (μg $L^{-1}$) | | | | | |
|---|---|---|---|---|---|---|---|---|---|---|
| | | | $SO_4^{2-}$ | $NO_3^-$ | Fe | Al | Mn | Zn | Ni | Cr |
| UA | 7 | 2.40 | 444 | 0.170 | 69,800 | 65,600 | 20,300 | 1200 | 617 | 10 |
| | | ±0.00943 | ±19.8 | ±0.0167 | ±4540 | ±4840 | ±1260 | ±78 | ±41 | ±0 |
| | 56 | 2.43 | 400 | 0.136 | 64,500 | 59,500 | 18,800 | 1120 | 563 | 10 |
| | | ±0.00471 | ±9.85 | ±0.0284 | ±454 | ±682 | ±122 | ±21 | ±5 | ±0 |
| TA | 7 | 2.60 | 349 | 0.156 | 64,500 | 67,800 | 20,200 | 1270 | 597 | 37 |
| | | ±0.0525 | ±13.2 | ±0.0217 | ±3170 | ±1670 | ±284 | ±60 | ±5 | ±12 |
| | 56 | 3.23 | 166 | 0.123 | 6550 | 36,600 | 10,600 | 620 | 293 | 23 |
| | | ±0.160 | ±17.4 | ±0.0206 | ±5602 | ±4000 | ±782 | ±43 | ±21 | ±5 |
| UM | 7 | 5.44 | 11.6 | 186 | 97 | 27 | 490 | 20 | 0 | 0 |
| | | ±0.0616 | ±0.724 | ±8.61 | ±9 | ±5 | ±16 | ±8 | ±0 | ±0 |
| | 56 | 5.67 | 9.94 | 162 | 140 | 27 | 177 | 70 | 0 | 0 |
| | | ±0.0170 | ±0.547 | ±6.68 | ±14 | ±5 | ±236 | ±42 | ±0 | ±0 |
| TM | 7 | 5.65 | 9.20 | 266 | 127 | 70 | 130 | 13 | 0 | 0 |
| | | ±0.800 | ±1.00 | ±39.4 | ±53 | ±37 | ±70 | ±9 | ±0 | ±0 |
| | 56 | 5.15 | 0.181 | 0.663 | 77 | 27 | 10 | 80 | 0 | 0 |
| | | ±0.0403 | ±0.0262 | ±0.0976 | ±37 | ±9 | ±14 | ±0 | ±0 | ±0 |

B) Physiological response of AMD and media grown vetiver

| Treatment | Time (days) | Change in biomass (%) | R:S | Total chlorophyll (mg $g^{-1}$) |
|---|---|---|---|---|
| AMD | 7 | −27.3 ± 2.19 | 0.47 ± 0.077 | 1.28 ± 0.200 |
| | 56 | −30.2 ± 6.47 | 0.40 ± 0.10 | 2.48 ± 0.667 |
| Media | 7 | −2.92 ± 3.06 | 0.30 ± 0.025 | 2.62 ± 0.336 |
| | 56 | 31.7 ± 1.32 | 0.40 ± 0.046 | 2.66 ± 0.375 |

C) Metal content (μg $g^{-1}$) of AMD and media grown vetiver tissues

| Treatment | Time (days) | Fe | | Al | | Mn | | Zn | | Ni | | Cr | |
|---|---|---|---|---|---|---|---|---|---|---|---|---|---|
| | | S | R | S | R | S | R | S | R | S | R | S | R |
| AMD | 7 | 671 | 3320 | 714 | 2337 | 397 | 244 | 47.6 | 55.3 | 6.99 | 5.63 | 2.66 | 23.5 |
| | | ±40.6 | ±647 | ±43.6 | ±1394 | ±94.9 | ±69.2 | ±6.80 | ±8.66 | ±0.818 | ±1.25 | ±0.468 | ±13.7 |
| | 56 | 1310 | 13,100 | 2720 | 4180 | 527 | 254 | 93.2 | 61.5 | 10.3 | 6.62 | 14.6 | 53.3 |
| | | ±299 | ±1960 | ±221 | ±2180 | ±55.8 | ±94.0 | ±6.99 | ±8.46 | ±0.447 | ±1.24 | ±3.84 | ±23.3 |
| Media | 7 | 57.9 | 946 | 71.1 | 1870 | 125 | 160 | 20.2 | 27.9 | 0.331 | 1.66 | 0.661 | 17.6 |
| | | ±5.95 | ±84.4 | ±10.3 | ±193 | ±54.3 | ±39.6 | ±2.47 | ±3.78 | ±0.468 | ±0.466 | ±0.468 | ±1.68 |
| | 56 | 118 | 1860 | 148 | 4110 | 71.2 | 317 | 28.8 | 53.9 | 0 | 1.99 | 1.98 | 37.6 |
| | | ±50.1 | ±1421 | ±83.6 | ±3228 | ±17.1 | ±124 | ±9.15 | ±21.3 | ±0 | ±0.812 | ±1.40 | ±28.5 |

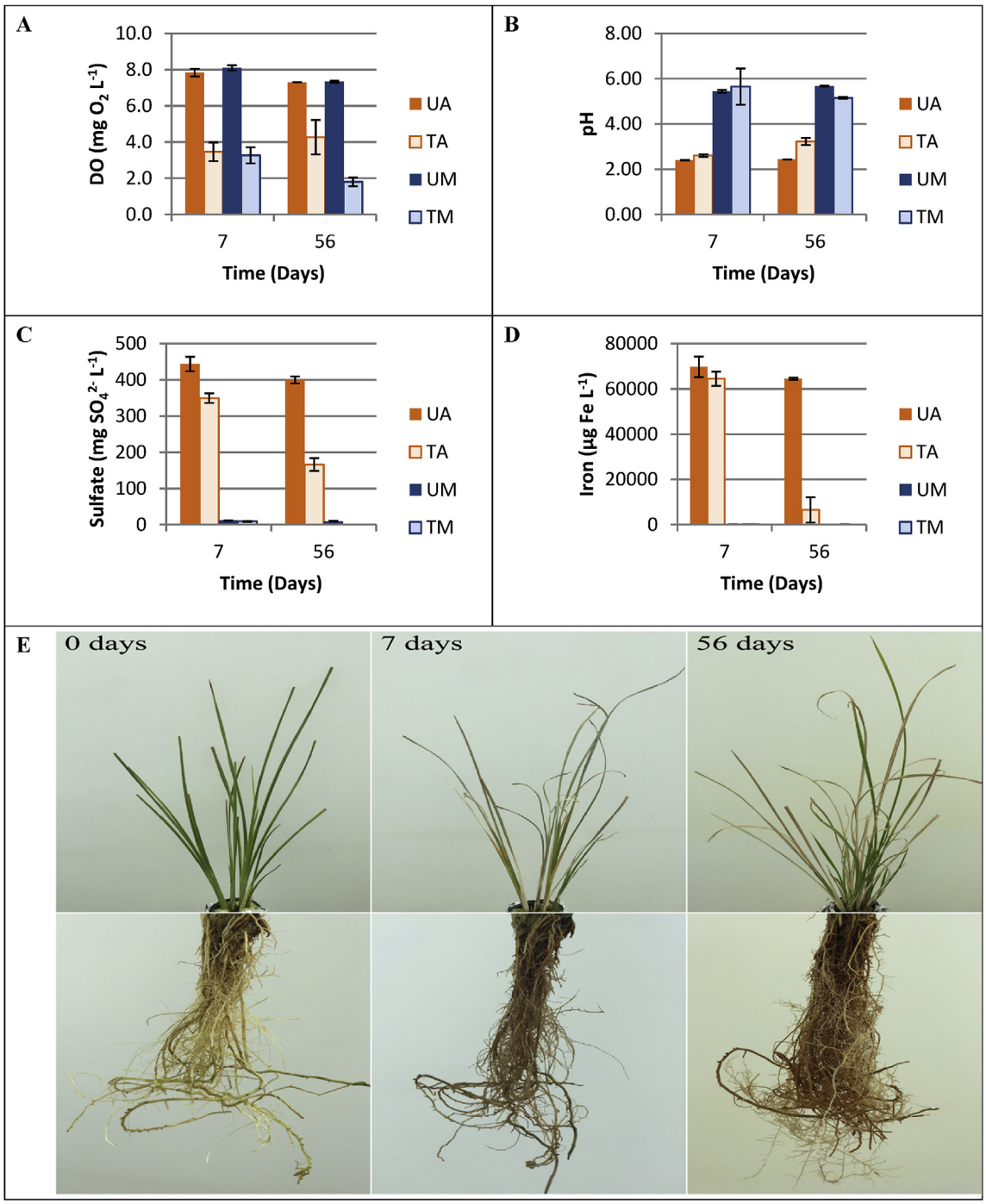


**Fig. 1.** Effect of vetiver on AMD and media for A) dissolved oxygen (DO), B) pH, C) $SO_4^{2-}$, and D) Fe among untreated AMD (UA), treated AMD (TA), untreated media (UM) and treated media (TM), and E) the appearance of AMD-grown vetiver shoots and roots at 0, 7, and 56 days. Numerical representations include mean ± standard deviation for n = 3 replicates.

observed in those roots that were not growing. These inhibitory effects were mitigated in the presence of Ca, suggesting that pectin polysaccharides are a major target of $H^+$ (Koyama et al., 2001). Reduced biomass and turgor loss were most noticeable in AMD-impacted vetiver, which suggested inhibited growth and dehydration resulted from a combination of metals and acidity. Osmotic imbalances from metals and ions could also have contributed to turgor loss of the shoots.

Metal hydroxides in AMD are suggested to have the greatest ecological impact of any stress factor, because they cover available surfaces while impairing normal functioning in organisms (Hogsden and Harding, 2012). Waterlogged plants allocate oxygen to the roots for cellular respiration (Pardo et al., 2016), releasing the excess into the rhizosphere as radial oxygen loss (Pardo et al., 2016; Li et al., 2017b). This leads to metal oxidation and precipitation, which collected as amorphous plaques along the root surfaces of vetiver (Li et al., 2017b). Therefore, it is likely that oxygen loss and root respiration contributed to the decreased dissolved oxygen and formation of root plaques. Moreover, the reduced uptake of essential resources and water would have exacerbated the stress

conditions (Pardo et al., 2016).

In addition to root damage and oxidative stress, vetiver was further deprived of essential alkaline nutrients like phosphorus and calcium from acidity and reduced solubility (Yan et al., 2015; van de Wiel et al., 2016). Furthermore, decreased pH also leads to an increase in the release of soluble metals. Plants generally increase their R:S ratios in response to nutrient deprivation, seeking to acquire more resources (Yan et al., 2015; van de Wiel et al., 2016). However, despite decreased biomass, growth of new and healthy green shoots, accompanied with abundant root growth and increased R:S ratios was observed in vetiver. The white solids on the shoot surface have been reported previously (Kiiskila et al., 2017) and are thought to be metals and excess $SO_4^{2-}$ that was exuded by the plants. However, further characterization of the exuded solids needs to be performed.

### 3.2. Metabolic profiling of vetiver shoots in response to AMD

Following 7 days, AMD-grown vetiver shoots exhibited differential regulation of eight metabolites, with seven upregulated and one downregulated. After 56 days, 61 metabolites showed differential regulation, with 47 upregulated and 14 downregulated. Most upregulated metabolites were amino acids (AAs), encompassing ornithine and its relatives, sulfur-containing AAs, and glutathione metabolism (Fig. 2A, Table S1). In addition, metabolites relating to cellular respiration and $C_4$ photosynthesis were upregulated (Fig. 2). Differential regulation of purine and phospholipid metabolism was also observed.

#### 3.2.1. Differential regulation of amino acid metabolism

*3.2.1.1. Upregulation of phenylalanine and downregulation of proline.* Differential regulation of the shikimate pathway was observed, involving decreased shikimate and increased phenylalanine at 56 days. There was upregulation of several AAs from the TCA cycle (Fig. 2A), including aspartate, threonine, glutamate, asparagine, histidine, alanine, and two branched chain AAs (BCAAs), leucine and isoleucine. Proline metabolism was downregulated, counting decreased 1-pyrroline-5-carboxylate at 7 and 56 days, and proline at 56 days.

Upregulation of AAs could relate to protein synthesis/degradation or more targeted responses. For instance, phenylalanine could have been used for lignin biosynthesis and strengthening cell walls (Sun et al., 2015), or for flavonoid biosynthesis through the phenylpropanoid pathway (Tohge et al., 2014; Sun et al., 2015). BCAAs have accumulated as osmolytes for drought stress or served as alternative electron donors for respiration (Sun et al., 2015).

Downregulation of proline and 1-pyrroline-5-carboxylate was not expected since proline is commonly upregulated in response to abiotic stresses (Xie et al., 2014; Slama et al., 2015; Winter et al., 2015; Chowra et al., 2017). Proline could have aided with cellular structure, protein stabilization (Slama et al., 2015), and ROS scavenging (Slama et al., 2015; Chowra et al., 2017). However, Mittler (2006) reported that proline is inhibited when drought conditions are combined with heat, emphasizing the importance of

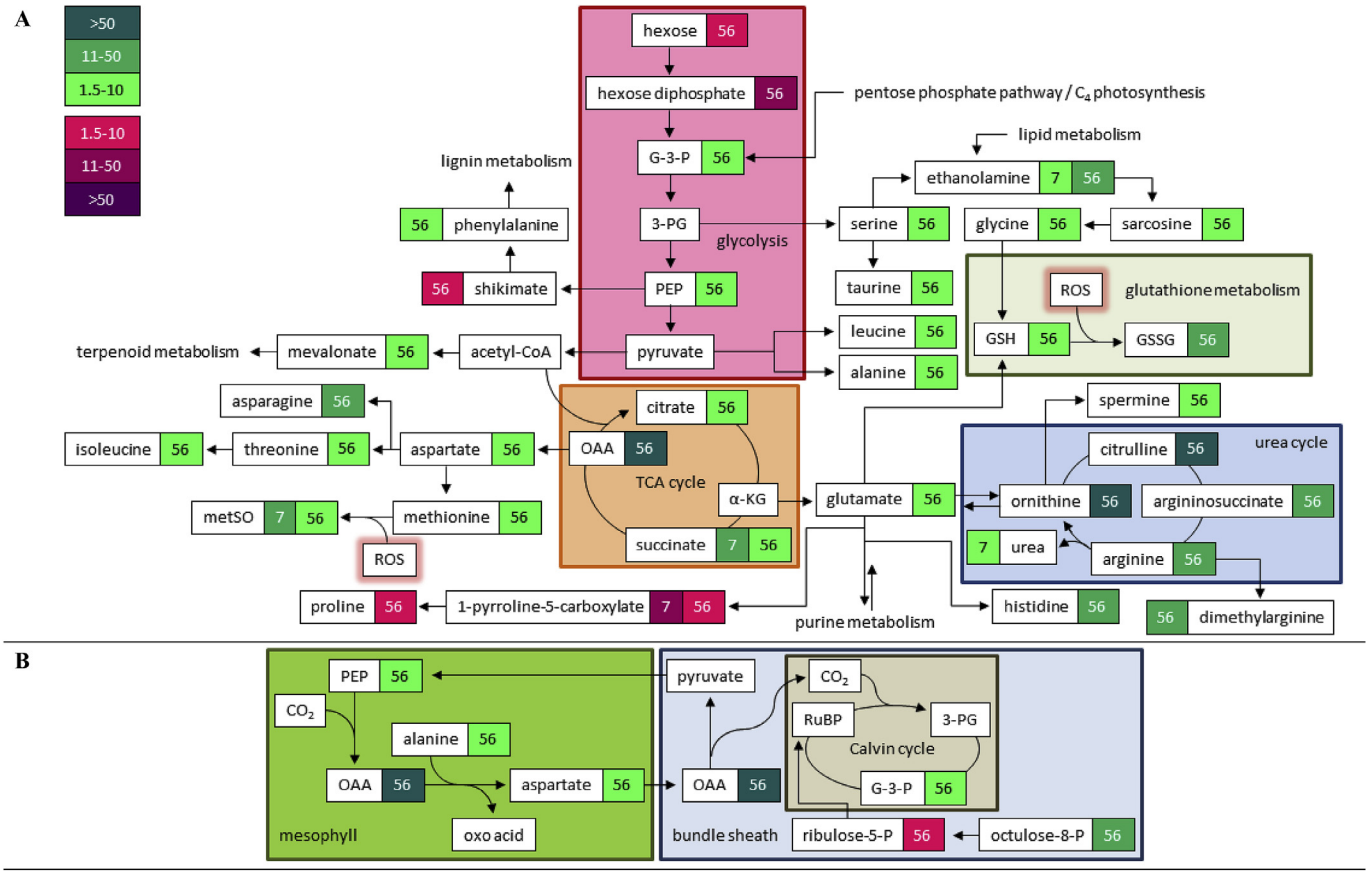


**Fig. 2.** Correlations of vetiver shoot metabolites in response to AMD, including A) pathways with regards to primary respiration and B) $C_4$ photosynthesis. Compounds of interest contain 7 and/or 56 to represent respective days of treatment, where green shading represents upregulation while magenta shading represents downregulation, including fold change increments for 1.5-to-10-fold, 11-to-50-fold, and >50- or 100-fold. (For interpretation of the references to colour in this figure legend, the reader is referred to the Web version of this article.)

investigating combined stresses or natural environments. This finding would suggest that proline was not significant to AMD-grown vetiver shoots as it is under most abiotic stress conditions.

*3.2.1.2. Upregulation of ornithine and related metabolites.* Metabolites of the urea cycle were significantly upregulated (Fig. 2A), where argininosuccinate increased 12-fold ($p = 0.004$), arginine increased 30-fold ($p = 0.002$), citrulline increased 71-fold ($p = 0.002$) and ornithine increased 207-fold ($p = 0.001$). Dimethylarginine, spermine, and ureidopropionate also increased. Interestingly, there was time-dependent downregulation of urea cycle AAs in media-grown vetiver, where argininosuccinate decreased 12-fold ($p = 0.008$), arginine decreased 13-fold ($p = 0.008$), citrulline decreased 14-fold ($p = 0.008$), and ornithine decreased 40-fold ($p = 0.004$). Therefore, AMD-grown vetiver accumulated and maintained higher levels of these metabolites while media-grown did not.

Arginine is used for storage and transport of organic nitrogen, containing the highest nitrogen-to-carbon ratio of proteogenic AAs (Winter et al., 2015), and also a nitric oxide precursor for signaling (Winter et al., 2015; Astier et al., 2017). Ornithine is a precursor to arginine that is synthesized in chloroplasts and has been thought to aid in drought tolerance (Winter et al., 2015). Given the significant upregulation of ornithine and its precursors, along with the lack of nitrogen in AMD, it is likely that vetiver used these metabolites as a source of nitrogen. Meanwhile, the media-grown vetiver had access to $NH_4^+$ and $NO_3^-$. Reactions from arginine or decarboxylation of ornithine could have generated polyamines such as spermine, which are important for their importance in development and general stress responses (Winter et al., 2015; Astier et al., 2017). Spermine was upregulated in AMD-grown vetiver, albeit not nearly as significantly as ornithine and its precursors.

*3.2.1.3. Upregulation of sulfur-containing amino acids and glutathione metabolism.* Sulfur was taken in by plant roots as $SO_4^{2-}$ and transported for assimilation into organic compounds (Pivato et al., 2014; Prodhan et al., 2017). Methionine increased 7.7-fold at 56 days ($p = 0.006$), and methionine sulfoxide (metSO) increased 16-fold at 7 days ($p = 0.014$) and 5.7-fold at 56 days ($p = 0.008$). Additionally, reduced glutathione (GSH) increased 3.0-fold ($p = 0.025$) at 56 days whereas oxidized glutathione (GSSG) increased 14-fold ($p = 0.004$). Additional GSH precursors included serine, ethanolamine, sarcosine, glycine, and taurine (Fig. 2A).

Methionine is one of two sulfur-containing, proteogenic AAs (Pivato et al., 2014). ROS readily oxidized methionine into metSO (Jacques et al., 2015; Zhu et al., 2015), which converted its hydrophobic *S*-methyl thioether into a polar group and likely misfolded proteins (Jacques et al., 2015). Given that metals and protons are known generators of oxidative stress, they must have had a cumulative effect in the upregulation of metSO in AMD-grown vetiver. However, differential changes showed that metSO was less upregulated at 56 days, suggesting that metSO was somewhat reduced back into its native state by vetiver.

Glutathione is a tripeptide with high reductive potential from cysteine and its free thiol (Das and Roychoudhury, 2014; Pivato et al., 2014). GSH is ideal for sulfur storage with long range transport capabilities (Pivato et al., 2014), but it is primarily used for ROS scavenging and phytochelatin biosynthesis (Andra et al., 2009; Das and Roychoudhury, 2014; Pivato et al., 2014; Liang et al., 2016). GSH is oxidized to GSSG, a dimer of glutathione that accumulates due to ROS scavenging under oxidative stress (Das and Roychoudhury, 2014; Pivato et al., 2014). Therefore, the GSH:GSSG ratio can function as an indicator of redox status (Das and Roychoudhury, 2014; Pivato et al., 2014). Glutathione can be used for the direct management of ROS; however, plants also use GSH to generate phytochelatins (Andra et al., 2009). Phytochelatins are large chains of glutathione that are used to bind metals, which are then transported into the cellular vacuoles in order to reduce intracellular damage (Andra et al., 2009; Hossain et al., 2012; Liang et al., 2016). Upregulation of GSSG, along with GSH, indicates that AMD-grown vetiver used GSH in order to directly manage oxidative stress.

Another interesting finding was the upregulation of taurine, which is not reportedly synthesized by plants. Taurine is derived from $SO_4^{2-}$ and serine, and is commonly used by algae to handle osmotic imbalances (Tevatia et al., 2015) and may have originated from microbial activity.

### 3.2.2. Upregulation of cellular respiration and photosynthesis metabolites

Upregulation of other TCA intermediates (Fig. 2A), including citrate and oxaloacetate (OAA), was observed at 56 days, where OAA increased 233-fold ($p = 0.001$). Succinate also increased at 7 and 56 days. Interestingly, OAA demonstrated a time-dependent, 57-fold decrease in media-grown vetiver by 56 days ($p = 0.004$). Early glycolytic intermediates were downregulated, including hexose sugars and hexose diphosphate sugars. Two later glycolytic intermediates were also upregulated, specifically glyceraldehyde-3-phosphate and phosphoenolpyruvate (PEP).

Photosynthetic decreases were evident early on, and were potentially related to inhibited carbon fixation or pigment breakdown from metals (Xie et al., 2014), or inhibited ribulose-1,5-bisphosphate regeneration from phosphorus deficiency (Yan et al., 2015). However, chlorophyll returned to normal at 56 days while photosynthetic metabolites such as octulose-phosphate, OAA, and PEP were upregulated (Williams and MacLeod, 2006). During $C_4$ photosynthesis, $CO_2$ is captured as OAA (Fig. 2B; Turkan et al., 2018) which is converted into a $C_4$-carrier (aspartate) and moved to the bundle sheath for reconversion to OAA (Turkan et al., 2018). OAA is then broken down to pyruvate and $CO_2$ for carbon fixation (Turkan et al., 2018). OAA was among the most highly upregulated metabolites, indicating that it plays a vital role to the shoots of AMD-grown vetiver. OAA is not reportedly upregulated in plants by metal stress, and has not been indicated for metal chelation. It is possible that OAA had a different function in vetiver. OAA is well known intermediate of the TCA cycle and cellular respiration, and likely served as a precursor for OA and AA synthesis (de la Torre-González, 2017). Furthermore, OAA has an integral role in $C_4$ photosynthesis (Turkan et al., 2018) where it could be used as a convenient form of carbon storage in the bundle sheath.

In addition, octulose-phosphate was upregulated 49-fold ($p = 0.002$) and functioned as a cycling intermediate of the pentose phosphate pathway for photosynthesis (Williams and MacLeod, 2006).

Organic acids (OAs) are commonly upregulated in response to metals (Xie et al., 2014; Chen and Liao, 2016) as their carboxy groups are able to partake in metal detoxification (Hossain et al., 2012; Xie et al., 2014). For instance, cytosolic chelation of $Al^{3+}$ under acidic conditions reportedly reduces toxicity while freeing up phosphorus (Chen and Liao, 2016). Succinate and OAA demonstrated greater upregulation in AMD-grown vetiver, which could simply as metabolic precursors. However, OAA is also thought to negate the effects of salinity by precipitating $Na^+$ (de la Torre-González, 2017).

Furthermore, a terpenoid precursor, mevalonate increased 5.7-fold ($p = 0.008$), suggesting upregulation of terpenoid biosynthesis (Durenne et al., 2018).

### 3.2.3. Purine and phospholipid metabolism in shoots

Purine and purine nucleosides were upregulated at 56 days,

including 3.0-to-8.4-fold increases in adenosine, deoxyadenosine, guanosine, deoxyguanosine, and xanthine (Table S1). Damaged purines, 1-methyladenosine and 1-methyladenine, were also upregulated. Conversely, there was downregulation of nucleotides inosine monophosphate, cyclic adenosine monophosphate (cAMP), and ribose-5-phosphate. Pyrimidines were largely unaffected, though thymidine increased 21-fold ($p = 0.003$).

Meanwhile, lipolysis intermediates of phosphatidylcholine (PC) increased at 7 days, comprising lysoPC(18:0), lysoPC(16:0), and linoleate, where the latter increased 24-fold ($p = 0.008$). Phospholipids were downregulated at 56 days, which included PC, phosphatidylglycerol (PG), and phosphatidylinositol (PI). Furthermore, there was a 44-fold increase in carnitine ($p = 0.002$) and a 49-fold increase in ethanolamine ($p = 0.002$). Although phospholipid downregulation was minor, upregulation of lysoPCs and fatty acids (FAs) suggested lipolysis with carnitine serving as a catabolic transporter.

Membrane damage from lipid peroxidation was possible (Das and Roychoudhury, 2014; Liang et al., 2016; Martinez et al., 2018), though no peroxidation products were detected. Phosphorus deprived plants rely on root uptake of $PO_4^{3-}$ and remobilization from older tissues (Yan et al., 2015; van de Wiel et al., 2016). Therefore, we hypothesized that vetiver utilized purine nucleotides, phosphorylated sugars, and phospholipids to remobilize $PO_4^{3-}$. Mature plant regions provided a potential source for actively growing vetiver tissues to recycle phosphorus (van de Wiel et al., 2016; Prodhan et al., 2017). Although the shoots dried from AMD exposure, vetiver gradually acclimated and fresh growth was observed. Remobilization of internal nitrogen and phosphorus would have facilitated the observed growth.

Resource remobilization and peroxidation requires replacement and/or remodeling of phospholipid membranes. Non-$PO_4^{3-}$ lipids would decrease need for $PO_4^{3-}$, increasing availability (Maejima et al., 2014). Plants have demonstrated replacement using glycolipids (Maejima et al., 2014), along with sulfolipids that served for sulfur storage (Pivato et al., 2014; van de Wiel et al., 2016). $SO_4^{2-}$ from AMD would provide a source for sulfolipid replacement, though this would need to be further investigated. Downregulated metabolites mainly contained $PO_4^{3-}$, suggesting a limited resource as expected from the low pH of AMD.

### 3.3. Metabolic profiling of vetiver roots in response to AMD

After 56 days, AMD-grown vetiver roots demonstrated differential regulation of 44 metabolites, with 40 downregulated and four upregulated (Table S1). There was differential regulation of 83 metabolites at 56 days, with 71 downregulated and 12 upregulated. More than half of the downregulated metabolites contained $PO_4^{3-}$, including 21 of 40 metabolites at 7 days and 34 of 71 at 56 days. Major pathways included phospholipid and purine metabolism, cellular respiration and glyoxylate metabolism, AA metabolism, and GSH (Fig. 3).

#### 3.3.1. Phospholipid and purine metabolism in roots

Root phospholipids were significantly impacted, where PG and four phosphatidylethanolamine (PE) decreased at 7 days (Fig. 3B). More significantly, three PI, three PG, four PC and six PE decreased 4.1-to-72-fold at 56 days. LysoPC(18:0) increased at 7 days and 56 days, whereas carnitine increased and linoleate increased at 56 days. Furthermore, phosphorylcholine decreased 70-fold at 7 days ($p = 0.014$) and 82-fold at 56 days ($p < 0.001$).

Nucleosides and nucleotides of adenine, guanine, uracil and xanthine were primarily downregulated but less than phospholipids. There was 2.4-to-13-fold downregulation of adenosine, AMP, deoxyadenosine, deoxyadenosine monophosphate, and cAMP at 56 days. 5-Methylthioadenosine decreased 14-fold at 7 days ($p = 0.039$) and 51-fold at 56 days ($p = 0.003$), while 1-methyladenine increased 4.5-fold at 56 days ($p = 0.034$). Pyrimidines were largely unaffected, though deoxycytidine diphosphate decreased 35-fold at 7 days ($p = 0.014$).

Roots contain negatively charged phospholipid membranes and pectin cell walls with carboxy groups, where metals could have bound and interfered with neutralizing cations (Maejima et al., 2014). For instance, Al reduces cell division and membrane integrity at the zone of elongation and root tips (Chowra et al., 2017), which could explain why fresh growth originated from the root-shoot transition of AMD-grown vetiver. AMD-derived plaques on vetiver roots primarily contained Fe and Al (Kiiskila et al., 2019), which are the two most abundant metals in Tab-Simco AMD. Plaques may have reduced internal toxicity, though they could have also interfered with resource acquisition (Hossain et al., 2012). Oxidative stress and lipid peroxidation are common with metals (Das and Roychoudhury, 2014; Liang et al., 2016; Chowra et al., 2017; Martinez et al., 2018). Therefore, the combination of oxidative stress and physical damage from metals and acidity could explain why phospholipid metabolism was so heavily affected in AMD-grown vetiver roots. Meanwhile, significant downregulation of other $PO_4^{3-}$ containing metabolites provided rationale for phosphorus remobilization (van de Wiel et al., 2016; Prodhan et al., 2017). It is obvious from the acidity of AMD that $PO_4^{3-}$ would not have been readily available until perhaps later in the treatment by AMD-grown vetiver. Therefore, vetiver would have resorted to recycling available phosphorus by remobilization from its own tissue, likely taking from the older and more damaged roots.

#### 3.3.2. Downregulation of cellular respiration and glyoxylate metabolism

Numerous respiration intermediates were downregulated, where fumarate, glyoxylate, isocitrate and citrate decreased at 7 days, along with malate, fumarate, and glyoxylate at 56 days (Fig. 3A). Sugar metabolism was generally downregulated, particularly 3-PG, PEP, ribose-phosphate, and fructose-phosphate decreased at 7 days, in addition to hexose sugars at 56 days. Moreover, sucrose-phosphate and *N*-acetylglucosamine-1-phosphate decreased at 7 and 56 days. Specifically, sucrose-phosphate decreased 54-fold at 7 days ($p < 0.001$) and 13-fold at 56 days ($p = 0.001$).

Hexose diphosphate sugars increased 13-fold ($p = 0.039$) and pyrophosphate increased 9.3-fold ($p = 0.013$) at 56 days. However, hexose diphosphate sugars decreased 42-fold ($p = 0.012$) while pyrophosphate decreased 26-fold ($p = 0.012$) in media-grown vetiver. There was downregulation of coenzyme metabolites, including pantothenate, riboflavin, flavin mononucleotide, flavin adenine dinucleotide and nicotinamide adenine dinucleotide (NAD).

Downregulation of OAs indicates root exudation, which is a common response to metals (Hossain et al., 2012; Chen and Liao, 2016; van de Wiel et al., 2016), $PO_4^{3-}$ deprivation (van de Wiel et al., 2016; Prodhan et al., 2017), and low pH (Hossain et al., 2012). OAs like citrate, fumarate and malate could have allowed for rhizospheric metal chelation (Hossain et al., 2012; Maejima et al., 2014; Chen and Liao, 2016; van de Wiel et al., 2016; Prodhan et al., 2017), and may have functioned for the pH adjustment that was observed with AMD-grown vetiver (Javed et al., 2013). For instance, it has been reported that Al-OA complexes from chelation reduce $Al^{3+}$ toxicity by 5-to-20-fold (Chen and Liao, 2016). Therefore, oxygen release and root exudates could have accounted for metal precipitation and formation of root plaques. Furthermore, OAs have lower affinity for pyrophosphate, which would have increased their availability (Chen and Liao, 2016).

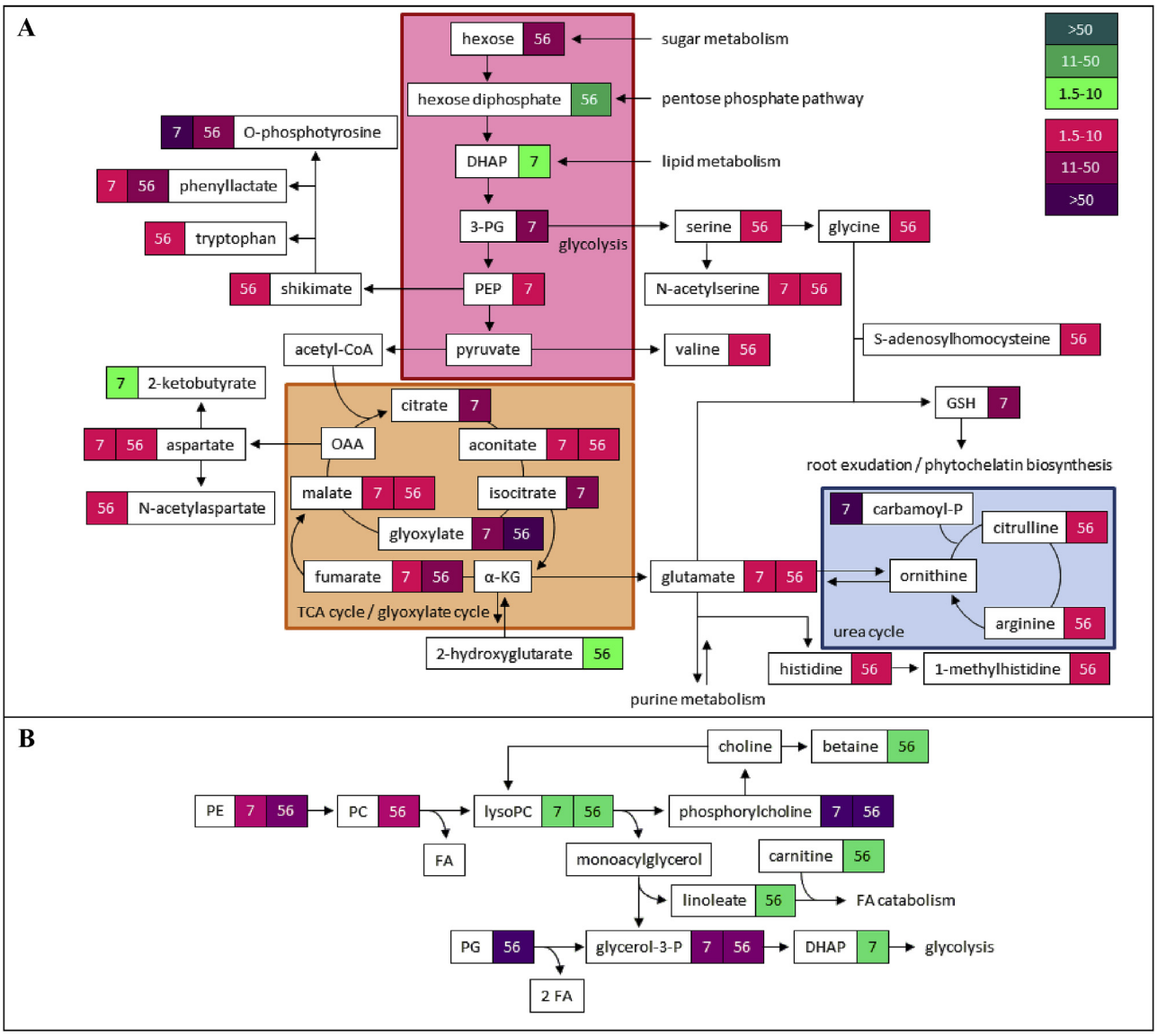


**Fig. 3.** Correlations of vetiver root metabolites in response to AMD, including A) pathways with regards to primary respiration and B) phospholipid metabolism. Compounds of interest contain 7 and/or 56 to represent respective days of treatment, where green shading represents upregulation while magenta shading represents downregulation, including fold change increments for 1.5-to-10-fold, 11-to-50-fold, and >50-fold. (For interpretation of the references to colour in this figure legend, the reader is referred to the Web version of this article.)

Upregulation of pyrophosphate and hexose diphosphate sugars at 56 days suggested that $PO_4^{3-}$ was more readily available in AMD-grown vetiver roots. Lastly, glyoxylate is a monocarboxylate and less functional as an exudate and more likely served in conversion of FAs to carbohydrates (Zarei et al., 2017).

### 3.3.3. Downregulation of amino acid metabolism and glutathione

Minor downregulation of AA metabolism was observed, including decreases in common AAs and a variety of intermediates, mainly phosphorylated (Fig. 3). For example, carbamoylphosphate decreased 301-fold at 7 days ($p = 0.010$), *O*-phosphotyrosine decreased 81-fold at 7 days ($p = 0.014$) and 38-fold at 56 days ($p = 0.004$). Additionally, GSH decreased 45-fold ($p = 0.037$) at 7 days. GSH decreased 29-fold ($p = 0.008$) in media-grown vetiver, whereas GSSG decreased 24-fold ($p = 0.049$).

Decreased carbamoylphosphate and *O*-phosphotyrosine likely resulted from phosphorus deprivation, where reduced downregulation at 56 days suggested that $PO_4^{3-}$ demands were better met. GSH was downregulated at 7 days while GSSG went unchanged, which indicates the potential of GSH being secreted as an exudate. Alternatively, GSH could have been used for phytochelatin biosynthesis or intracellular chelation (Das and Roychoudhury, 2014; Pivato et al., 2014; Liang et al., 2016). Time-dependent downregulation of glutathione in media-grown vetiver was unexpected but potentially explained by lower $SO_4^{2-}$ and less demand for GSH. AMD-grown vetiver had a surplus of $SO_4^{2-}$ at 56 days while GSH was in higher demand for stress management.

### 3.4. Metabolic profiling of root exudates and rhizospheric metabolites in response to AMD

Only a few metabolites were within detection limits in the AMD in which vetiver was grown (Table S2). Thirty of the metabolites were either higher or only detected in the presence vetiver. There

were nine OAs, including aconitate, succinate, citrate, and isocitrate of the TCA cycle, along with derivatives that consisted of citramalate, 2-hydroxyglutarate, 2-isopropylmalate, methylsuccinate, and 2-methylcitrate. These metabolites showed some of the highest increases in AMD. The majority of TCA OAs were downregulated in the roots; however, there were specific correlation with aconitate, citrate, and isocitrate from the root exudates.

Four exudates were directly related to phospholipid metabolism; including *O*-phosphoethanolamine, linoleate, ethanolamine, and glycerol. Additional exudates included six sugars, three AAs, two nucleosides, and a variety of miscellaneous metabolites. Out of the sugars, hexose-phosphate and erythrose-phosphate increased the greatest, which correlated with the downregulation of sugar metabolism in the roots. Increased adenosine correlated with the downregulation of root adenosine and adenosine nucleotides, such as AMP and ADP. Increased proline was not correlated to root downregulation, though it is possible that proline was transported from the shoots.

Carboxy-containing metabolites like AAs or FAs could have functioned for metal chelation and precipitation (Hossain et al., 2012; Maejima et al., 2014; Chen and Liao, 2016; van de Wiel et al., 2016; Prodhan et al., 2017). Increased aconitate, citrate, and isocitrate in AMD could have explained their downregulation in the roots, and suggested that these particular OAs were released into the rhizosphere by vetiver.

Carboxy- and amine-containing metabolites, such as *O*-phosphoethanolamine and ethanolamine could have influenced pH of the AMD (Javed et al., 2013). Shifts in pH have also been observed following exudation of inorganic anions like $PO_4^{3-}$ (Hossain et al., 2012). Moreover, increased pyrophosphate could have been an indicator that phosphorus solubility had improved as previously hypothesized. Since proline in the shoot was downregulated, increased proline levels in AMD was unexpected, though it likely functioned for ROS scavenging (Slama et al., 2015; Chowra et al., 2017). Long-range transport from the shoots and exudation from the roots could explain the downregulation of shoot proline.

## 4. Conclusions

Our study showed considerable differential metabolism in AMD-grown vetiver, including upregulation of shoot metabolites after longer-term exposure and a general downregulation of root metabolites. The shoots demonstrated changes to AA and glutathione metabolism, along with cellular respiration and photosynthetic pathways. In particular, there was significant accumulation of ornithine, thought to have functioned for nitrogen storage, along with OAA, which could have had multiple functions. Changes in OAs and glutathione levels were likely related to oxidative stress and metal chelation, which would have aided in tolerance. Meanwhile, the roots demonstrated contrasting changes in AA metabolism along with cellular respiration and glyoxylate metabolism. Several OAs that were downregulated in the roots were also detected in the AMD, which indicated that they were secreted from the roots. Secreted metabolites could have functioned for metal chelation, pH adjustment, or osmoregulation but these avenues need to be further explored. Both tissues (roots significantly more than the shoots) demonstrated downregulation of phosphorylated metabolites such as phospholipids and phosphorylated sugars. Phosphorus deprivation would have accompanied the acidity of AMD; therefore we hypothesize that phosphorylated metabolites were recycled for their $PO_4^{3-}$ groups. These findings have shed light on the molecular responses of vetiver to Tab-Simco AMD.

## Declarations of interest

None.

## Author contributions

Jeffrey Kiiskila: Investigation, validation, formal analysis and writing original draft; Kefeng Li: Metabolomics sample analysis and interpretation; Dibyendu Sarkar: Funding acquisition, resources, conceptualization; Rupali Datta: Funding acquisition, resources, conceptualization; supervision, project administration, data interpretation, writing (review and editing).

## Acknowledgements

The Office of Surface Mining Reclamation and Enforcement is acknowledged for funding this study (Grant #S12AC20001). Authors thank Saumik Panja for performing ion and metal analyses. Additional thanks to Yi Cui, Mona Fabian, Reginald Mullen, Alexus Rule, Nikki Saari, and Amanda Turcotte for assistance in the greenhouse and laboratory.

## Appendix A. Supplementary data

Supplementary data to this article can be found online at https://doi.org/10.1016/j.chemosphere.2019.124961.

## References

Andra, S.S., Datta, R., Sarkar, D., Makris, K.C., Mullens, C.P., Sahi, S.V., Bach, S.B.H., 2009. Induction of lead-binding phytochelatins in vetiver grass [vetiveria zizanioides (L.)]. J. Environ. Qual. 38, 868–877.

Arnon, D., 1949. Copper enzymes in isolated chloroplasts: polyphenylperoxydase in *Beta vulgaris*. Plant Physiol. 24 (1), 1–15.

Astier, J., Gross, I., Durner, J., 2017. Nitric oxide production in plants: an update. J. Exp. Bot. https://doi.org/10.1093/jxb/erx420.

Chen, Z.C., Liao, H., 2016. Organic acid anions: an effective defensive weapon for plants against aluminum toxicity and phosphorus deficiency in acidic soils. J. Genet. Genom. 43, 631–638.

Chowra, U., Yanase, E., Koyama, H., Panda, S.K., 2017. Aluminium-induced excessive ROS causes cellular damage and metabolic shifts in black gram Vigna mungo (L.) Hepper. Protoplasma 254, 293–302.

Das, K., Roychoudhury, A., 2014. Reactive oxygen species (ROS) and response of antioxidants as ROS-scavengers during environmental stress in plants. Front. Environ. Sci. 2 (53), 1–13.

de la Torre-González, A., Albacete, A., Sánchez, E., Blasco, B., 2017. Comparative study of the toxic effect of salinity in different genotypes of tomato plants: carboxylates metabolism. Sci. Hortic. 217, 173–178.

De Vos, R.C.H., Moco, S., Lommen, A., Keurentjes, J.J.B., Bino, R.J., Hall, R.D., 2007. Untargeted large-scale plant metabolomics using liquid chromatography coupled to mass spectrometry. Nat. Protoc. 2 (4), 778–791.

Durenne, B., Blondel, A., Druart, P., Fauconnier, M.-L., 2018. A laboratory high-throughput glass chamber using dynamic headspace TD-GC/MS method for the analysis of whole *Brassica napus* L. plantlet volatiles under cadmium-related abiotic stress. Phytochem. Anal. 29, 463–471.

Hogsden, K.L., Harding, J.S., 2012. Consequences of acid mine drainage for the structure and function of benthic stream communities: a review. Freshw. Sci. 31 (1), 108–120.

Hossain, M.A., Piyatida, P., Teixeira da Silva, J.A., Fujita, M., 2012. Molecular mechanism of heavy metal toxicity and tolerance in plants: central role of glutathione in detoxification of reactive oxygen species and methylglyoxal and in heavy metal chelation. J. Bot. 1–37.

Jacques, S., Ghesquiére, B., De Bock, P.-J., Demol, H., Wahni, K., Willems, P., Messens, J., Van Breusegem, F., Gevaert, K., 2015. Protein methionine sulfoxide dynamics in Arabidopsis thaliana under oxidative stress. Mol. Cell. Proteom. 14 (5), 1217–1229.

Javed, M.T., Stoltz, E., Lindberg, S., Greger, M., 2013. Changes in pH and organic acids in mucilage of Eriophorum angustifolium roots after exposure to elevated concentrations of toxic elements. Environ. Sci. Pollut. Control Ser. 20 (3), 1876–1880.

Karathanasis, A.D., Johnson, C.M., 2003. Metal removal potential by three aquatic plants in an acid mine drainage wetland. Mine Water Environ. 22 (1), 22–30.

Kiiskila, J.D., Sarkar, D., Feuerstein, K.A., Datta, R., 2017. A preliminary study to design a floating treatment wetland for remediating acid mine drainage-impacted water using vetiver grass (*Chrysopogon zizanioides*). Environ. Sci. Pollut. Control Ser. 24 (36), 27985–27993.

Kiiskila, J.D., Sarkar, D., Panja, S., Sahi, S.V., Datta, R., 2019. Remediation of acid mine drainage-impacted water by vetiver grass (*Chrysopogon zizanioides*): a multi-scale long-term study. Ecol. Eng. 129, 97–108.

Koyama, H., Toda, T., Hara, T., 2001. Brief exposure to low-pH stress causes irreversible damage to the growing root in Arabidopsis thaliana: pectin-Ca interaction may play an important role in proton rhizotoxicity. J. Exp. Bot. 52 (355), 361–368.

Lager, I., Andréasson, O., Dunbar, T., Andreasson, E., Escobar, M.A., Rasmusson, A.G., 2010. Changes in external pH rapidly alter plant gene expression and modulate auxin and elicitor responses. Plant Cell Environ. 33 (9), 1513–1528.

Li, K., Pidatala, V.R., Shaik, R., Datta, R., Ramakrishna, W., 2014. Integrated metabolomic and proteomic approaches dissect the effect of metal-resistant bacteria on maize biomass and copper uptake. Environ. Sci. Technol. 48, 1184–1193.

Li, L., Chen, X., Shi, L., Wang, C., Fu, B., Qiu, T., Cui, S., 2017a. A proteome translocation response to complex desert stress environments in perennial phragmites sympatric ecotypes with contrasting water availability. Front. Plant Sci. 8, 1–15.

Li, W.C., Deng, H., Wong, M.H., 2017b. Effects of Fe plaque and organic acids on metal uptake by wetland plants under drained and waterlogged conditions. Environ. Pollut. 231, 732–741.

Liang, T., Ding, H., Wang, G., Kang, J., Pang, H., Lv, J., 2016. Sulfur decreases cadmium translocation and enhances cadmium tolerance by promoting sulfur assimilation and glutathione metabolism in *Brassica chinensis* L. Ecotoxicol. Environ. Saf. 124, 129–137.

Ma, L., Rao, X., Lu, P., Huang, S., Chen, X., Xu, Z., Xie, J., 2015. Acid-tolerant plant species screened for rehabilitating acid mine drainage sites. J. Soils Sediments 15 (5), 1104–1112.

Maejima, E., Watanabe, T., Osaki, M., Wagatsuma, T., 2014. Phosphorus deficiency enhances aluminum tolerance of rice (Oryza sativa) by changing the physiological characteristics of root plasma membranes and cell walls. J. Plant Physiol. 171, 9–15.

Martinez, V., Nieves-Cordones, M., Lopez-Delacalle, M., Rodenas, R., Mestre, T.C., Garcia-Sanchez, F., Rubio, F., Nortes, P.A., Mittler, R., Rivero, R.M., 2018. Tolerance to stress combination in tomato plants: new insights in the protective role of melatonin. Molecules 23, 1–20.

Mittler, R., 2006. Abiotic stress, the field environment and stress combination. Trends Plant Sci. 11 (1), 15–19.

Pardo, T., Martinez-Fernandez, D., Fuente, C., Clemente, R., Komarek, M., Bernal, M.P., 2016. Maghemite nanoparticles and ferrous sulfate for the stimulation of iron plaque formation and arsenic immobilization in Phragmites australis. Environ. Pollut. 219, 296–304.

Pidatala, V.R., Li, K., Sarkar, D., Wusirika, R., Datta, R., 2016. Identification of biochemical pathways associated with lead tolerance and detoxification in *Chrysopogon zizanioides* L. Nash (vetiver) by metabolic profiling. Environ. Sci. Technol. 50, 2530–2537.

Pidatala, V.R., Li, K., Sarkar, D., Wusirika, R., Datta, R., 2018. Comparative metabolic profiling of vetiver (*Chrysopogon zizanioides*) and maize (*Zea mays*) under lead stress. Chemosphere 193, 903–911.

Pivato, M., Fabrega-Prats, M., Masi, A., 2014. Low-molecular-weight thiols in plants: functional and analytical implications. Arch. Biochem. Biophys. 560, 83–99.

Prodhan, M.A., Jost, R., Watanabe, M., Hoefgen, R., Lambers, H., Finnegan, P.M., 2017. Tight control of sulfur assimilation: an adaptive mechanism for a plant from a severely phosphorus-impoverished habitat. New Phytol. 215, 1068–1079.

RoyChowdhury, A., Sarkar, D., Datta, R., 2015. Remediation of acid mine drainage-impacted water. Current Pollut. Rep. 1, 131–141.

Shavrukov, Y., Hirai, Y., 2016. Good and bad protons: genetic aspects of acidity stress responses in plants. J. Exp. Bot. 67 (1), 15–30.

Slama, I., Abdelly, C., Bouchereau, A., Flowers, T., Savouré, A., 2015. Diversity, distribution and roles of osmoprotective compounds accumulated in halophytes under abiotic stress. Ann. Bot. 115, 433–447.

Sun, C., Gao, X., Fu, J., Zhou, J., Wu, X., 2015. Metabolic response of maize (Zea mays L.) plants to combined drought and salt stress. Plant Soil 388, 99–117.

Tevatia, R., Allen, J., Rudrappa, D., White, D., Clemente, T.E., Cerutti, H., Demirel, Y., Bluma, P., 2015. The taurine biosynthetic pathway of microalgae. Algal Res. 9, 21–26.

Tohge, T., Obata, T., Fernie, A.R., 2014. Biosynthesis of the essential respiratory cofactor ubiquinone from phenylalanine in plants. Mol. Plant 7, 1403–1405.

Turkan, I., Uzilday, B., Dietz, K.-J., Bräutigam, A., Ozgur, R., 2018. Reactive oxygen species and redox regulation in mesophyll and bundle sheath cells of C4 plants. J. Exp. Bot. https://doi.org/10.1093/jxb/ery064.

van de Wiel, C.C.M., van der Linden, C.G., Scholten, O.E., 2016. Improving phosphorus use efficiency in agriculture: opportunities for breeding. Euphytica 207, 1–22.

Williams, J.F., MacLeod, J.K., 2006. The metabolic significance of octulose phosphates in the photosynthetic carbon reduction cycle in spinach. Photosynth. Res. 90, 125–148.

Winter, G., Todd, C.D., Trovato, M., Forlani, G., Funck, D., 2015. Physiological implications of arginine metabolism in plants. Front. Plant Sci. 6, 1–14.

Xie, Y., Hu, L., Du, Z., Sun, X., Amombo, E., Fan, J., Fu, J., 2014. Effects of cadmium exposure on growth and metabolic profile of bermudagrass [*Cynodon dactylon* (L.) pers.]. PLoS One 9 (12), 1–20.

Yan, N., Zhang, Y.-L., Xue, H.-M., Zhang, X.-H., Wang, Z.-D., Shi, L.-Y., Guo, D.-P., 2015. Changes in plant growth and photosynthetic performance of *Zizania latifolia* exposed to different phosphorus concentrations under hydroponic condition. Photosynthetica 53 (4), 630–635.

Zarei, A., Brikis, C.J., Bajwa, V.S., Chiu, G.Z., Simpson, J.P., DeEll, J.R., Bozzo, G.G., Shelp, B.J., 2017. Plant glyoxylate/succinic semialdehyde reductases: comparative biochemical properties, function during chilling stress, and subcellular localization. Front. Plant Sci. 8, 1–13.

Zhu, J., Ding, P., Li, Q., Gao, Y., Chen, F., Xia, G., 2015. Molecular characterization and expression profile of methionine sulfoxide reductase gene family in maize (*Zea mays*) under abiotic stresses. Gene 562, 159–168.